The Journal of Veterinary Medical Science

NOTE

Surgery

Magnetic resonance imaging findings of an intradural extramedullary hemangiosarcoma in a dog

Kenji KUTARA[1)], Noritaka MAETA[1)]*, Teppei KANDA[1)], Akihiro OHNISHI[1)], Ikki MITSUI[1)], Masahiro MIYABE[1)], Yuki SHIMIZU[1)] and Yasuhiko OKAMURA[1)]

[1)]Faculty of Veterinary Medicine, Okayama University of Science, 1-3 Ikoinooka, Imabari, Ehime 794-8555, Japan

J. Vet. Med. Sci.
81(10): 1527–1532, 2019
doi: 10.1292/jvms.19-0260

Received: 14 May 2019
Accepted: 19 August 2019
Advanced Epub:
4 September 2019

ABSTRACT. An 11-year-old male Miniature Dachshund was referred for acute neurological deficits in the pelvic limbs. T2-weighted magnetic resonance imaging revealed that the spinal cord at the L1-2 intervertebral disc space was heterogeneously hyperintense in the sagittal plane and was mildly compressed from the ventral side by a small hypointense mass in the transverse plane. However, the lesion showed mass enhancement and severe spinal cord compression on post-contrast T1-weighted imaging. On three-dimensional myelography, a "golf tee sign" was observed around the mass. Therefore, we diagnosed an intradural extramedullary lesion. The mass was surgically removed and histologically diagnosed as a hemangiosarcoma. The "golf tee sign" observed on magnetic resonance myelography may be useful for distinguishing intradural extramedullary masses from intramedullary masses.

KEY WORDS: intradural extramedullary tumor, hemangiosarcoma, magnetic resonance imaging, magnetic resonance myelography, whole-body computed tomography

Neurological deficits of the pelvic limbs occur due to various causes, including intervertebral disc herniation and neoplasia of the spinal cord [2, 5]. Intervertebral disc herniation often causes acute spasmodic gait, whereas neoplasia of the spinal cord often causes chronic and progressive signs [2, 5]. Magnetic resonance imaging (MRI) is commonly used to characterize spinal cord lesions in dogs.

Neoplasia of the spinal cord can be classified as extradural and intradural extramedullary or intramedullary. Of these, extradural tumors are the most prevalent type in dogs, accounting for approximately half of all cases. Intradural extramedullary tumors comprise one-third of cases and intramedullary tumors the remainder [8]. Common intradural extramedullary tumors include meningioma, neuroblastoma, and nerve sheath tumors [12]. Intradural extramedullary tumors have characteristic MRI findings, such as thickened meningeal enhancement and enhancement of the peripheral margin of the mass and dura ("dural tail sign") [6, 10, 17]. Previous studies have reported that the presence of a "golf tee sign" on MRI also suggests an intradural extramedullary lesion [6, 10, 16].

Hemangiosarcoma is a rare spinal cord tumor, and extradural and intramedullary hemangiosarcomas have been reported [3, 7]. The extradural form can arise from the vertebrae, accounting for approximately 2 to 3% of primary bone tumors of the vertebral column in dogs [11]. Rarely, hemangiosarcoma can affect the epidural space. Intramedullary hemangiosarcoma is usually metastatic, while the vertebral and epidural forms are typically primary tumors [11]. To the authors' knowledge, MRI findings of intradural extramedullary hemangiosarcoma have not been reported in dogs.

This report describes for the first time MRI findings of intradural extramedullary hemangiosarcoma. It also demonstrates that a "golf tee sign" on MRI is a significant sign of an intradural extramedullary tumor when the typical MRI findings of intradural extramedullary tumors, including meningeal enhancement and a "dural tail sign," are not evident.

An 11-year-old male Miniature Dachshund, weighing 4.16 kg, was referred to Okayama University of Science Veterinary Medical Teaching Hospital with acute neurological deficits in the pelvic limbs. Neurologic examination revealed severe ambulatory paraparesis with absent conscious proprioception in both pelvic limbs and normal segmental spinal reflexes. Deep pain perception had disappeared, but urination was possible. Spinal hyperesthesia was elicited upon palpation of the caudal thoracic spine, and a T3-L3 myelopathy was suspected. Other clinical findings were normal. No significant abnormalities were identified on the complete blood cell count, serum biochemistry, and thoracic radiographs. The main differential diagnoses were intervertebral disc disease, neoplasia, inflammatory disease, and vascular disorder (infarction).

*Correspondence to: Maeta, N.: n-maeta@vet.ous.ac.jp

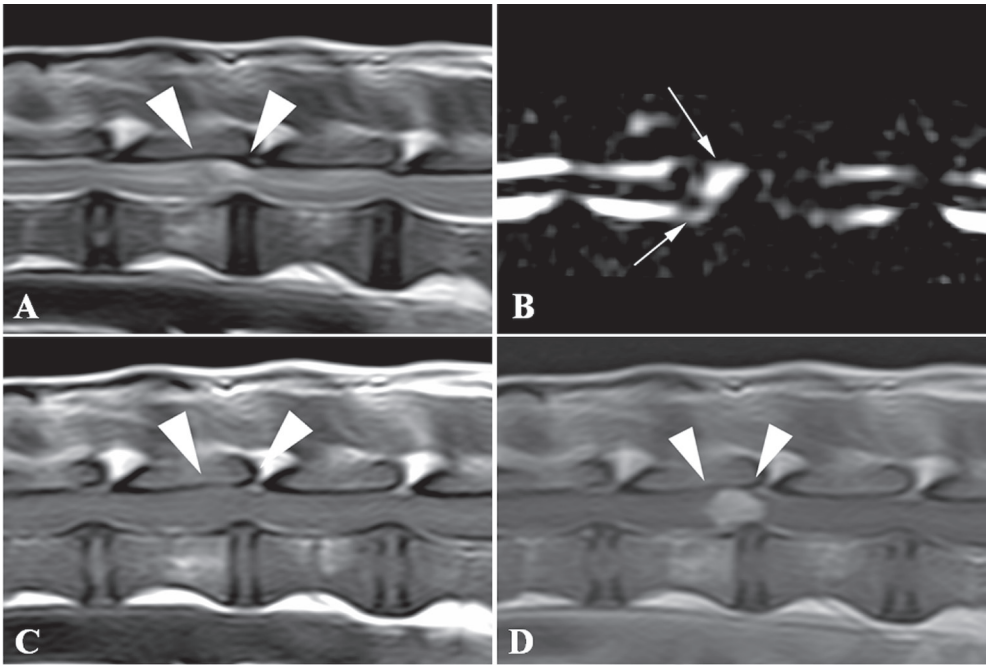

Fig. 1. Magnetic resonance images in the sagittal plane showing the mass lesion (white arrowheads). (A) T2-weighted image. The spinal cord at the level of the L1-2 intervertebral disc space shows a heterogeneously hyperintense lesion. (B) Three-dimensional myelography image. The margins of the mass are within the intradural extramedullary compartment, and the ventral cerebrospinal fluid line is deviated dorsally, creating the "golf tee sign" (white arrows). (C) T1-weighted image. (D) Post-contrast T1-weighted image. The entire mass displays contrast enhancement.

MRI was performed with a 1.5 T superconducting unit (Vantage Elan, Canon Medical Systems, Otawara, Japan). Technical parameters included the following: T1-weighted [repetition time (TR)=350 msec, echo time (TE)=15 msec, field of view (FOV)=250 × 200 mm, thickness=2.5 mm, spatial resolution=0.5 × 0.25 mm] and T2-weighted (TR=2,500 msec, TE=80 msec, FOV=250 × 200 mm, thickness=2.5 mm, spatial resolution=0.5 × 0.25 mm) images in the sagittal plane; T1-weighted (TR=600 msec, TE=10 msec, FOV=80 × 80 mm, thickness=2 mm, spatial resolution=0.3 × 0.3 mm) and T2-weighted (TR=3,850 msec, TE=121 msec, FOV=80 × 80 mm, thickness=2 mm, spatial resolution=0.3 × 0.3 mm) images in the transverse plane; and T1-weighted (TR=350 msec, TE=15 msec, FOV=150 × 150 mm, thickness=2 mm, spatial resolution=0.3 × 0.3 mm) and T2-weighted (TR=2,500 msec, TE=80 msec, FOV=150 × 150 mm, thickness=2 mm, spatial resolution=0.3 × 0.3 mm) images in the dorsal plane. Three-dimensional magnetic resonance (MR) myelography [single-shot fast spin echo sequence (SS-FSE); TR=4,000 msec, TE=510 msec, FOV=200 × 200 mm, thickness=1 mm, spatial resolution=0.25 × 0.25 mm] was also performed. In addition, T1-weighted images (T1WI) in the sagittal, transverse, and dorsal planes were obtained after intravenous administration of contrast medium [0.2 m/kg bodyweight, gadodiamide (Omniscan; Daiichi-Sankyo Co., Tokyo, Japan)].

On the sagittal plane of the T2-weighted images (T2WI), the spinal cord showed a heterogeneously hyperintense lesion at the level of the L1-2 intervertebral disc space (Fig. 1A). On T2WI in the transverse plane, the lesion was hyperintense and mildly compressed from the ventral side by a small hypointense mass (Fig. 2A). However, on MR myelography in the sagittal plane (Fig. 1B), the spinal cord was severely compressed from the ventral side by the mass. The margins of the mass were within the intradural extramedullary compartment, and the ventral cerebrospinal fluid line was deviated dorsally, creating the so-called "golf tee sign" suggestive of an intradural extramedullary lesion. Furthermore, on post-contrast T1WI, the mass was enhanced (mass size: 3 × 4 ×6 mm), and the spinal cord was compressed from the right side at the cranial part of the L1-2 segment (Figs. 1C, 1D 2B, and 2C). However, thickened meningeal enhancement and a "dural tail sign" were not evident. In addition, a mass (size: 8 × 8 ×15 mm) was found in the right multifidus lumborum of the L2-3 vertebrae (Fig. 3). The mass had a hypointense central region and a hyperintense peripheral region on T2WI and post-contrast T1WI. The mass was not connected to the previously mentioned spinal cord mass. Based on the MRI findings, we suspected an intradural extramedullary neoplasia or intradural disc herniation. Therefore, whole-body computed tomography (CT) was performed to screen for possible metastases with a 16-slice multi slice CT scanner (Aquilion™ Lightning, Canon Medical Systems, Otawara, Japan). Technical parameters included the following: rotation time=0.75 sec; slice thickness=1 mm; reconstruction interval=0.5 mm; table speed=16 mm/rotation; helical pitch=16.0; X-ray tube voltage=120 kV; and X-ray tube current=100 mA. On the CT images, the left side of the spinal cord showed a hyper-attenuated lesion at the level of the L1-2 (Fig. 4A). Moreover, small masses (4–12 mm) were scattered in the subcutaneous tissues throughout the body (Fig. 4B). Furthermore, small masses (3–5 mm) were also scattered in the lungs (Fig. 4C). Masses were not found in other organs, including the liver, spleen, and right atrium. A large primary tumor was not found; however, we considered the possibility of multiple tumors and metastases based on imaging findings. Contrast enhanced CT was not performed because the owner did not

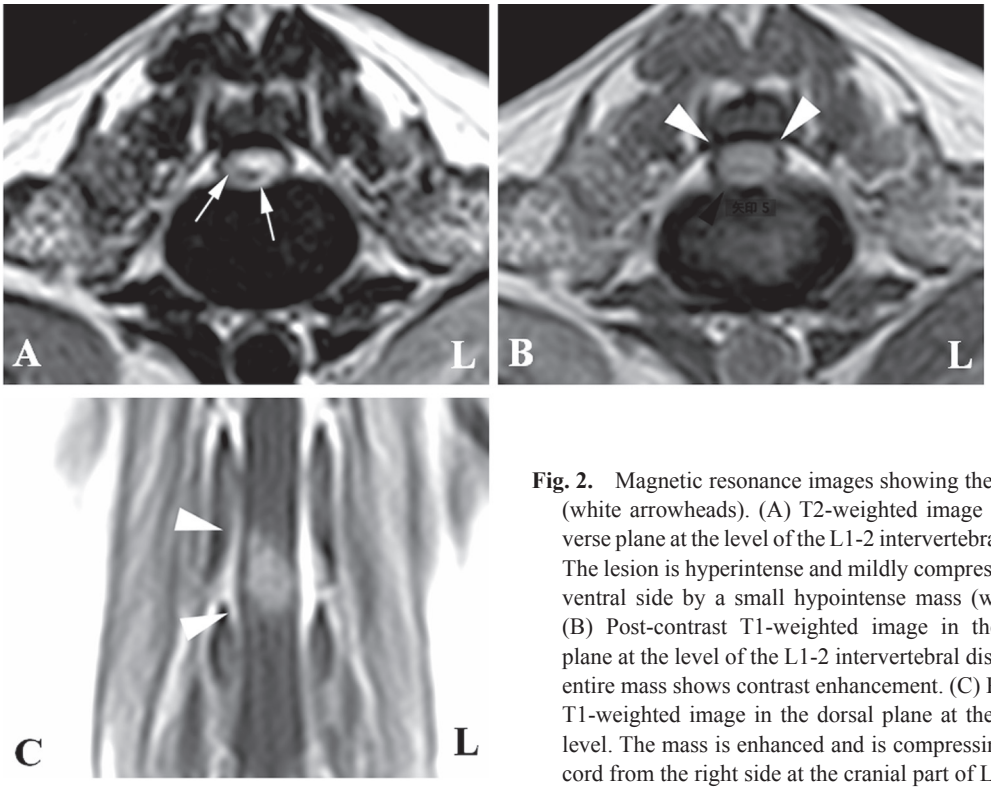

Fig. 2. Magnetic resonance images showing the mass lesion (white arrowheads). (A) T2-weighted image in the transverse plane at the level of the L1-2 intervertebral disc space. The lesion is hyperintense and mildly compressed from the ventral side by a small hypointense mass (white arrow). (B) Post-contrast T1-weighted image in the transverse plane at the level of the L1-2 intervertebral disc space. The entire mass shows contrast enhancement. (C) Post-contrast T1-weighted image in the dorsal plane at the spinal cord level. The mass is enhanced and is compressing the spinal cord from the right side at the cranial part of L1-2.

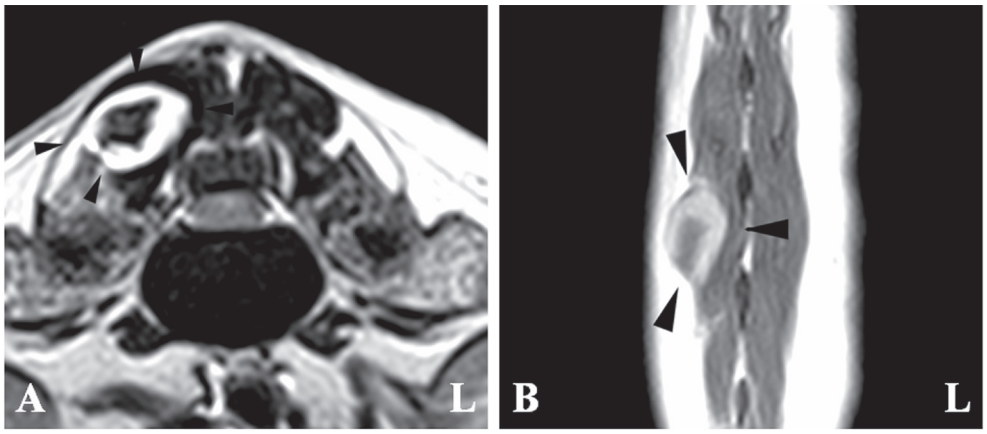

Fig. 3. Magnetic resonance images. (A) T2-weighted image in the transverse plane at the level of the L2-3 intervertebral disc space. (B) Post-contrast T1-weighted image in the dorsal plane of the mass. A mass (black arrowheads) is present in the right multifidus lumborum and has a hypointense central region and hyperintense peripheral region.

approve it due to financial considerations.

After discussing the imaging findings with the owner, hemilaminectomy and durotomy were performed in an attempt to improve the pelvic limb paraparesis.

After the mass in the right multifidus lumborum was removed, a right-sided hemilaminectomy was performed over the affected vertebral arch. No evidence of an epidural mass was found (Fig. 5A); however, a focal spinal cord swelling was observed. A durotomy was performed in this area, and the spinal cord was injured, revealing a red mass (Fig. 5B). The mass was not adhered and was removed easily from the intradural extramedullary space. After the mass's removal, mild hemorrhage occurred but stopped immediately. The resected mass, which was well-circumscribed, dark red to grey in color, and appeared elastic (Fig. 6A), was submitted for histopathological evaluation.

Histologically, both the intradural extramedullary tumor and the tumor from the right multifidus lumborum were characterized by anastomosing slits and cavernous spaces lined by atypical endothelial cells (Fig. 6B and 6C). The neoplastic cells contained scant eosinophilic cytoplasm, a moderately anisokaryotic ovoid euchromatic nucleus, and a distinct nucleolus. The mitotic count

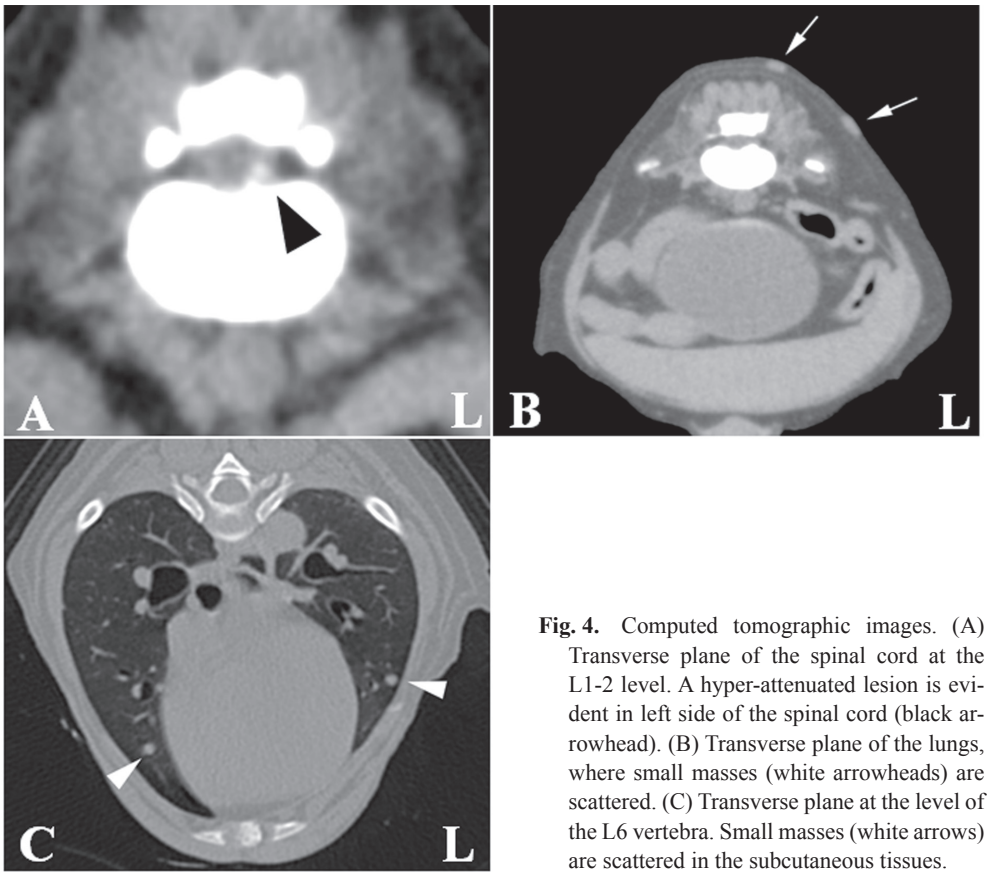

Fig. 4. Computed tomographic images. (A) Transverse plane of the spinal cord at the L1-2 level. A hyper-attenuated lesion is evident in left side of the spinal cord (black arrowhead). (B) Transverse plane of the lungs, where small masses (white arrowheads) are scattered. (C) Transverse plane at the level of the L6 vertebra. Small masses (white arrows) are scattered in the subcutaneous tissues.

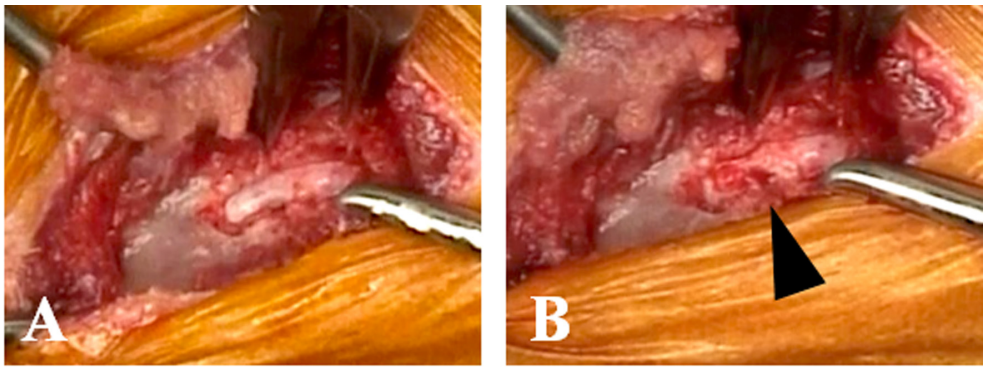

Fig. 5. Intraoperative photographs. (A) A right-side hemilaminectomy is performed over the affected vertebral arch. No evidence of an epidural mass is found. However, a focal spinal cord swelling is observed. (B) After a durotomy is performed, the spinal cord is injured, and a red mass is found (black arrowhead).

was 14 per ten 400× fields, using an ocular field number of 22. Hemorrhage and necrosis were frequent within the masses. These findings were consistent with hemangiosarcoma.

Two weeks postoperatively, the pelvic limb paraparesis had not improved. The segmental spinal reflexes were slightly diminished, but urination was possible. Deep pain perception did not recover. The owner declined further treatment, and we were missing about the progress because the patient did not return to the clinic.

To our knowledge, this is the first report describing the MRI characteristics of an intradural extramedullary hemangiosarcoma in a dog. Hemangiosarcoma is a highly malignant tumor derived from an endothelial cell line that can potentially arise in any site with blood vessels, and it frequently metastasizes [3, 11]. The most common primary sites of this tumor are the spleen and right atrium [3, 14]. Myelopathies in dogs associated with hemangiosarcoma are usually the result of primary or metastatic vertebral bone hemangiosarcoma invading the vertebral canal and compressing the spinal cord [3, 11]. In this case, small masses were found in the spinal cord and muscle, along with the subcutaneous tissues and lungs. However, a primary tumor was not found in

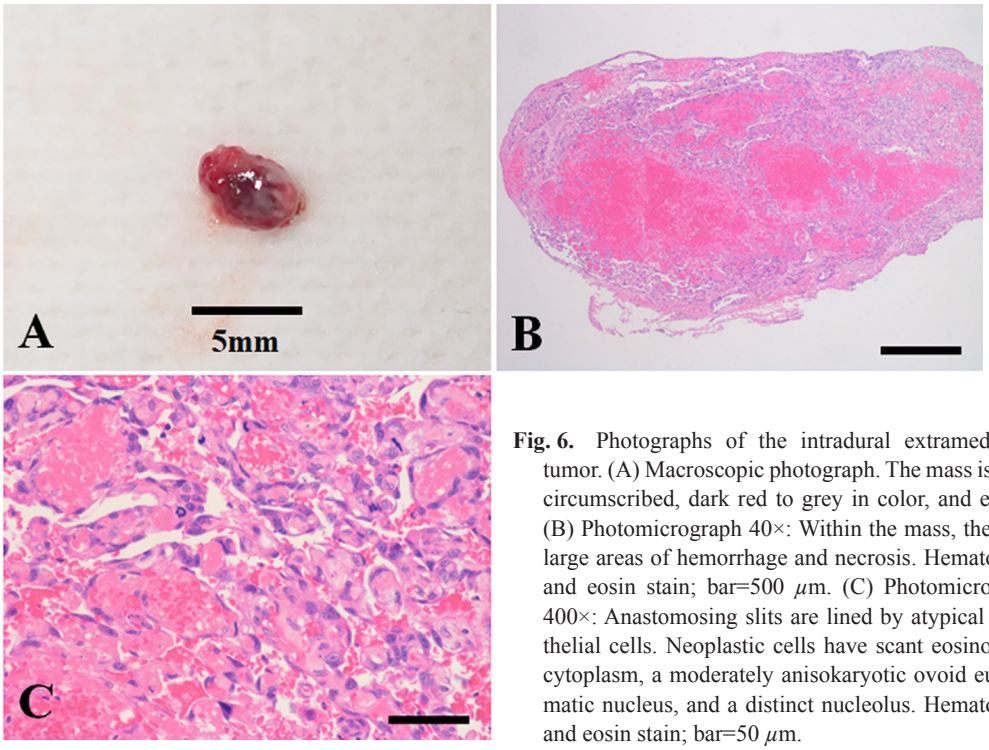

Fig. 6. Photographs of the intradural extramedullary tumor. (A) Macroscopic photograph. The mass is well-circumscribed, dark red to grey in color, and elastic. (B) Photomicrograph 40×: Within the mass, there are large areas of hemorrhage and necrosis. Hematoxylin and eosin stain; bar=500 μm. (C) Photomicrograph 400×: Anastomosing slits are lined by atypical endothelial cells. Neoplastic cells have scant eosinophilic cytoplasm, a moderately anisokaryotic ovoid euchromatic nucleus, and a distinct nucleolus. Hematoxylin and eosin stain; bar=50 μm.

other locations, including the liver, spleen, right atrium, and vertebral bone. In this case, the largest tumor was located in the right multifidus lumborum, but the size of this tumor was approximately 1cm, which was too small to determine the primary site. Hence, the primary site of the tumor could not be located. The tumor in the spinal cord was suspected to be a metastatic lesion that was causing the acute pelvic limb paraparesis.

The MRI findings of spinal hemangiosarcoma have been reported. Previous reports of spinal hemangiosarcoma have described epidural, extradural and intramedullary hemangiosarcomas, including metastases [3, 4, 7]. From these findings, spinal hemangiosarcomas appear as hyperintense lesions on T2WI and isointense in the remainder of the spinal cord on T1WI. Additionally, in contrast T1WI, the lesions display contrast enhancement. In extradural hemangiosarcoma, compression of the spinal cord by the tumor was shown, and the boundary between the spinal cord and the tumor was clearly discernable on T2WI, T1WI, and contrast T1WI [3]. In this case, a clear boundary between the spinal cord and the tumor could not be observed. Further, the T2WI, T1WI, and contrast T1WI findings of this case appeared to be the same with those of intramedullary hemangiosarcoma as reported by a previous study [4]. In the previous report [4], intramedullary hemangiosarcoma did not show a "golf tee sign" in MR myelography (SS-FSE). Hence, the "golf tee sign" observed on MR myelography (SS-FSE) may be useful for distinguishing intradural extramedullary hemangiosarcoma from intramedullary hemangiosarcoma. In this case, the "golf tee sign" observed on MR myelography (SS-FSE) was useful for diagnosing the intradural extramedullary lesion. According to previous reports, the "golf tee sign" might be an indicator of an intradural extramedullary lesion, including intradural disc herniation, on T2WI, T1WI, and heavy T2WI [6, 7, 16]. In this case, the affected spinal cord showed a heterogeneously hyperintense lesion, and the "golf tee sign" was unclear in the sagittal plane on T2WI but clear on MR myelography. MR myelography (SS-FSE) showed only cerebrospinal fluid because of the lack of signal from any substance except pure fluid [13]. Therefore, MR myelography may be useful for cases in which the "golf tee sign" is unclear on T2WI, such as those where the spinal cord appears heterogeneous due to tumor, edema, and inflammation. The typical MRI findings of intradural extramedullary tumors, including meningioma, histiocytic sarcoma, and leptomeningeal oligodendrogliomatosis, are medullary masses, thickened meningeal enhancement, and the "dural tail sign" [6, 10, 11, 17]. Furthermore, nerve sheath tumors extend peripherally to the intervertebral foramen in the form of an elongated mass [11]. In this case, a medullary mass was observed, but the other typical tumor findings were not present. Hence, when only a medullary mass is found, MR myelography should be performed.

Differentiating an intradural extramedullary tumor from an intradural disc herniation based on the acute clinical signs and MRI findings was also difficult in this case. Intervertebral disc herniation is a common disorder in dogs that mainly affects chondrodystrophoid breeds, including Miniature Dachshunds [1]. In intradural disc herniation, which is rare in dogs, an extruded nucleus pulposus penetrates the dura matter [16]. In this case, medullary mass enhancement and severe spinal cord compression were shown on post-contrast T1WI. However, a lesion was present in the intervertebral disc space, and mild compression from the ventral side by a small hypointense mass was shown on T2WI. Hence, it was difficult to determine whether an intradural extramedullary tumor or intradural disc herniation was present. In a previous report, contrast enhancement of compressive material was shown in 51.5% of intervertebral disc herniations [15]. It was suggested that contrast enhancement of compressive material

should not be interpreted as a specific sign of a mass, such as neoplasia. Therefore, we performed a whole-body CT examination to screen for metastases and other tumors. As a result, multiple small tumors were identified in the subcutaneous tissues of the entire body and in the lungs. Hence, we discussed the possibility of a malignant tumor and metastases with the owner. Therefore, it is important to perform both MRI and CT in patients with acute neurological deficits in the pelvic limbs.

In this case, there was a hyper-attenuated lesion on CT in the left side of the spinal cord at the L1-2 level. Hyper-attenuation findings may suggest acute hemorrhage [18]. However, hyper-attenuation in the spinal cord reflected compressing material in intradural disc herniation [9]. On MRI, hemorrhage appears as a hypointense lesion in T2WI and T2*-weighted gradient re-called echo sequence images [4]. Furthermore, in these images, intramedullary hemangiosarcoma appeared as a focal hypointense lesion [4]. In this case, a T2*-weighted gradient re-called echo sequence image was not obtained. Moreover, we performed CT after the MRI examination. When a hyper-attenuated lesion in the spinal cord is observed on CT and a focal hypointense lesion is observed on T2WI, it is important to obtain T2*-weighted gradient re-called echo images to distinguish hemorrhagic diseases, including hemangiosarcoma, from intradural disc herniation.

In conclusion, this report presented the findings of an intradural extramedullary hemangiosarcoma, which were the same as those of intramedullary hemangiosarcoma, on the general MR sequence including T2WI, T1WI, and contrast T1WI. Moreover, the typical MRI findings of the other intradural extramedullary tumors were not observed. The "golf tee sign" observed on MR myelography (SS-FSE) was only able to distinguish intradural extramedullary hemangiosarcoma from intramedullary hemangiosarcoma. Furthermore, this case illustrates that the "golf tee sign" observed on MR myelography (SS-FSE) is useful for distinguishing an intradural extramedullary lesion from an intramedullary lesion, even when this sign is unclear on the T2WI sagittal plane. This case also highlights that when a spinal cord tumor is suspected, it is important to determine if metastases and other masses are present using whole-body CT.

ACKNOWLEDGMENTS. The authors thank Dr. Yasuhito Hongu of Hongu Animal Hospital for providing this case. This study had no source of funding or conflict of interest.

REFERENCES

1. Bartels, K. E., Higbee, R. G., Bahr, R. J., Galloway, D. S., Healey, T. S. and Arnold, C. 2003. Outcome of and complications associated with prophylactic percutaneous laser disk ablation in dogs with thoracolumbar disk disease: 277 cases (1992–2001). *J. Am. Vet. Med. Assoc.* **222**: 1733–1739. [Medline] [CrossRef]
2. Costa, R. C. and Platt, S. R. 2017. Spinal cord diseases: congenital (developmental), inflammatory and degenerative disorders. pp. 1428–1442. *In*: Textbook of Veterinary Internal Medicine, 8th ed. (Ettinger, S. J., Feldman, E. C. and Cote, E. eds.), Elsevier, St. Louis.
3. de la Fuente, C., Pumarola, M. and Añor, S. 2014. Imaging diagnosis-spinal epidural hemangiosarcoma in a dog. *Vet. Radiol. Ultrasound* **55**: 424–427. [Medline] [CrossRef]
4. Hammond, L. J. and Hecht, S. 2015. Susceptibility artifacts on T2*-weighted magnetic resonance imaging of the canine and feline spine. *Vet. Radiol. Ultrasound* **56**: 398–406. [Medline] [CrossRef]
5. Jeffery, N. 2017. Spinal cord diseases: Traumatic, vascular, and neoplastic disorders. pp. 1443–1451. *In*: Textbook of Veterinary Internal Medicine, 8th ed. (Ettinger, S. J., Feldman, E. C. and Cote, E. eds.), Elsevier, St. Louis.
6. José-López, R., de la Fuente, C., Pumarola, M. and Añor, S. 2013. Spinal meningiomas in dogs: description of 8 cases including a novel radiological and histopathological presentation. *Can. Vet. J.* **54**: 948–954. [Medline]
7. Kippenes, H., Gavin, P. R., Bagley, R. S., Silver, G. M., Tucker, R. L. and Sande, R. D. 1999. Magnetic resonance imaging features of tumors of the spine and spinal cord in dogs. *Vet. Radiol. Ultrasound* **40**: 627–633. [Medline] [CrossRef]
8. LeCouteur, R. A. 2001. Tumors of the nervous system. pp. 514–531. *In*: Small Animal Clinical Oncology, 3rd ed. (Withrow, S. J. and MacEvan, E. G. eds.), WB Saunders, Philadelphia.
9. Lim, C., Kweon, O. K., Choi, M. C., Choi, J. and Yoon, J. 2010. Computed tomographic characteristics of acute thoracolumbar intervertebral disc disease in dogs. *J. Vet. Sci.* **11**: 73–79. [Medline] [CrossRef]
10. Lobacz, M. A., Serra, F., Hammond, G., Oevermann, A. and Haley, A. C. 2018. Imaging diagnosis-magnetic resonance imaging of diffuse leptomeningeal oligodendrogliomatosis in a dog with "dural tail sign". *Vet. Radiol. Ultrasound* **59**: E1–E6. [Medline] [CrossRef]
11. Mai, W. 2018. Magnetic resonance imaging and computed tomography features of canine and feline spinal cord disease. pp. 271–304. *In*: Textbook of Veterinary Diagnostic Radiology, 7th ed. (Thrall, D. E. ed.), Elsevier, St. Louis.
12. Masciarelli, A. E., Griffin, J. F. 4th., Fosgate, G. T., Hecht, S., Mankin, J. M., Holmes, S. P., Platt, S. R., Kent, M., Pancotto, T. E., Chen, A. V. and Levine, J. M. 2017. Evaluation of magnetic resonance imaging for the differentiation of inflammatory, neoplastic, and vascular intradural spinal cord diseases in the dog. *Vet. Radiol. Ultrasound* **58**: 444–453. [Medline] [CrossRef]
13. Pease, A., Sullivan, S., Olby, N., Galano, H., Cerda-Gonzalez, S., Robertson, I. D., Gavin, P. and Thrall, D. 2006. Value of a single-shot turbo spin-echo pulse sequence for assessing the architecture of the subarachnoid space and the constitutive nature of cerebrospinal fluid. *Vet. Radiol. Ultrasound* **47**: 254–259. [Medline] [CrossRef]
14. Smith, A. N. 2003. Hemangiosarcoma in dogs and cats. *Vet. Clin. North Am. Small Anim. Pract.* **33**: 533–552, vi. [Medline] [CrossRef]
15. Suran, J. N., Durham, A., Mai, W. and Seiler, G. S. 2011. Contrast enhancement of extradural compressive material on magnetic resonance imaging. *Vet. Radiol. Ultrasound* **52**: 10–16. [Medline]
16. Tamura, S., Doi, S., Tamura, Y., Takahashi, K., Enomoto, H., Ozawa, T. and Uchida, K. 2015. Thoracolumbar intradural disc herniation in eight dogs: clinical, low-field magnetic resonance imaging, and computed tomographic myelography findings. *Vet. Radiol. Ultrasound* **56**: 160–167. [Medline] [CrossRef]
17. Taylor, A., Eichelberger, B., Hodo, C., Cooper, J. and Porter, B. 2015. Imaging diagnosis--spinal cord histiocytic sarcoma in a dog. *Vet. Radiol. Ultrasound* **56**: E17–E20. [Medline] [CrossRef]
18. Zarelli, M., Shiel, R., Gallagher, B., Skelly, C., Cahalan, S. and McAllister, H. 2012. Imaging diagnosis: CT findings in a dog with intracranial hemorrhage secondary to angiostrongylosis. *Vet. Radiol. Ultrasound* **53**: 420–423. [Medline] [CrossRef]